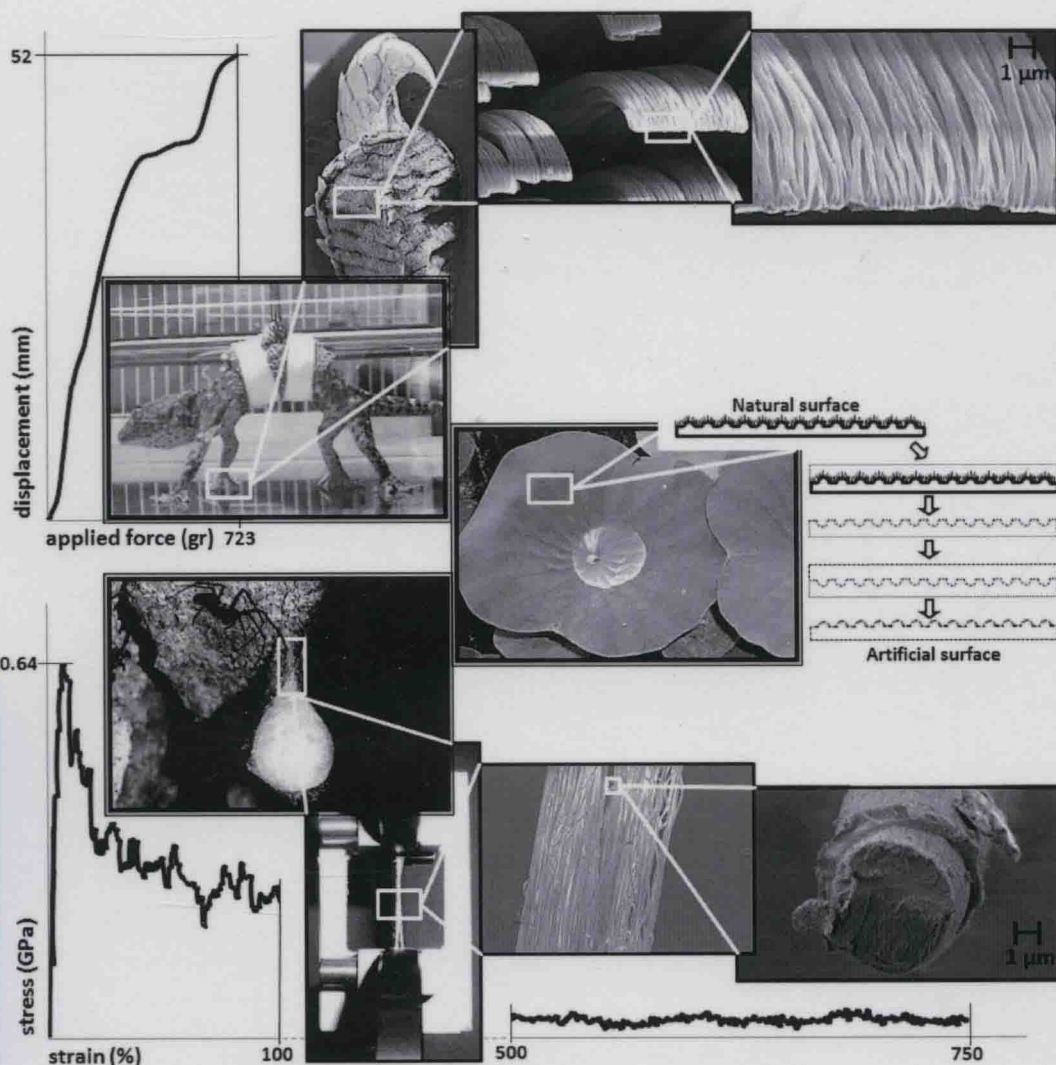


An Experimental Study on Adhesive or Anti-adhesive, Bio-inspired Experimental Nanomaterials

Emiliano Lepore, Nicola Pugno



Emiliano **Lepore**
Nicola **Pugno**

An Experimental Study on Adhesive or Anti-adhesive, Bio-inspired Experimental Nanomaterials



VERSITA

Published by Versita, Versita Ltd, 78 York Street, London W1H 1DP, Great Britain.



This work is licensed under the Creative Commons Attribution-NonCommercial-NoDerivs 3.0 license, which means that the text may be used for non-commercial purposes, provided credit is given to the author.

Copyright © 2013 Emiliano Lepore, Nicola Pugno

ISBN (paperback): 978-83-7656-080-9

ISBN (hardcover): 978-83-7656-081-6

ISBN (for electronic copy): 978-83-7656-082-3

Managing Editor: Elisa Capello

Language Editor: Mary Boyd

www.versita.com

Cover illustration: © Emiliano Lepore

*Dedicated to
small things which become great*

3800251

Versita Discipline: Engineering, Industry, Transportation

Managing Editor:

Elisa Capello

Language Editor:

Mary Boyd

Published by Versita, Versita Ltd, 78 York Street, London W1H 1DP, Great Britain.



This work is licensed under the Creative Commons Attribution-NonCommercial-NoDerivs 3.0 license, which means that the text may be used for non-commercial purposes, provided credit is given to the author.

Copyright © 2013 Emiliano Lepore, Nicola Pugno

ISBN (paperback): 978-83-7656-080-9

ISBN (hardcover): 978-83-7656-081-6

ISBN (for electronic copy): 978-83-7656-082-3

Managing Editor: Elisa Capello

Language Editor: Mary Boyd

www.versita.com

Cover illustration: © Emiliano Lepore

Contents

Acknowledgements.....	11
List of Figures	13
List of Tables	19
General Introduction.....	21
Adhesive Materials	23
Chapter 1	
The Weibull Statistics Applied to the Adhesion Times of Living Tokay Geckos on Nanorough Surfaces	25
Abstract.....	25
1.1. Introduction.....	25
1.2. Surface Characterization	27
1.3. Weibull Statistics.....	34
1.3.1. The First Set of Experiments.....	34
1.3.2. The Second Set of Experiments	39
1.4. Conclusions.....	41
Chapter 2	
The Gecko's Optimal Adhesion on Nanorough Surfaces	43
Abstract.....	43
2.1. Introduction.....	43
2.2. Materials and Methods.....	45
2.3. Results and Conclusions.....	46

Chapter 3

Normal Adhesive Force-Displacement Curves of Living Tokay Geckos.... 51

Abstract.....	51
3.1. Introduction.....	51
3.2. Materials and Methods.....	52
3.2.1. Gecko's Feet Architecture.....	52
3.2.2. PMMA and Glass Surface Characterization.....	54
3.2.3. The Gecko's Normal Adhesive Force <i>versus</i> Displacement Curves	54
3.3. Results.....	57
3.3.1. The Gecko's Feet Architecture.....	57
3.3.2. PMMA and Glass Surface Characterization.....	58
3.3.3. The Gecko's Normal Adhesive Force <i>versus</i> Displacement curves	58
3.4. Discussion.....	60
3.4.1. Feet Damage	61
3.5. Conclusions.....	62

Chapter 4

Optimal Angles for Maximal Adhesion in Living Tokay Geckos 63

Abstract.....	63
4.1. Introduction.....	63
4.2. Materials and Methods.....	65
4.3. Results	67
4.4. Discussion.....	68
4.5. Conclusions.....	70

Chapter 5

Observations of Shear Adhesive Force and Friction of *Blatta Orientalis* on Different Surfaces 71

Abstract.....	71
5.1. Introduction.....	71
5.2. Experimental Set-up	73
5.3. Video Output.....	75
5.4. AFM Characterization of Surfaces.....	76
5.5. FESEM Characterization of <i>Blatta Orientalis</i>	77
5.6. sSF Evaluation.....	77
5.7. Experimental Results.....	78
5.8. Discussion	78
5.9. Conclusions.....	81

Anti-Adhesive Materials	83
--------------------------------------	-----------

Chapter 6

Plasma and Thermoforming Treatments to Tune The Bio-Inspired Wettability of Polystyrene.....	85
---	-----------

Abstract.....	85
6.1. Introduction.....	85
6.2. Materials and Methods.....	86
6.2.1. Plasma Treatment.....	86
6.2.2. Thermoforming Treatment	87
6.2.3. Surface Characterization.....	87
6.2.4. CA Measurement.....	88
6.2.5. Sliding Measurements.....	88
6.3. Results.....	89
6.3.1. Surface Characterization	89
6.3.2. CA Measurement.....	89
6.3.3. Sliding Measurements.....	89
6.4. Discussion.....	101
6.4.1. Plasma Treatment.....	101
6.4.2. Thermoforming Treatment: Adhesive Static and Resistant Forces	104
6.5. Conclusions.....	105

Chapter 7

A Superhydrophobic Polystyrene by Replicating the Natural Lotus Leaf.....	107
--	------------

Abstract.....	107
7.1. Introduction.....	107
7.2. Materials and Methods.....	109
7.2.1 Molding Method.....	109
7.2.2. Surface Characterization.....	111
7.2.3. Wettability Measurement.....	111
7.3. Results.....	112
7.3.1. Surface Characterization	112
7.3.2. Wettability Measurement.....	112
7.4. Discussion.....	114
7.5. Conclusions.....	116

Strong Materials	117
-------------------------------	------------

Chapter 8
Evidence of the Most Stretchable Egg Sac Silk Stalk of the European Spider of the Year *Meta Menardi*..... 119

Abstract.....119

8.1. Introduction.....119

8.2. Materials and Methods.....124

 8.2.1. Tensile Testing124

 8.2.2. FESEM and FIB Characterization126

8.3. Results.....127

8.4. Discussion.....130

8.5. Conclusion143

Bibliography.....145

Final Acknowledgments167

General Conclusions169

Index173

Acknowledgements

First and foremost, I would like to express my deep gratitude to my tutor Prof. Nicola Pugno for his theoretical rigour and fascinating scientific approach. I thank Nature for its continuous stimulus and inspiration to optimization.

I wish to sincerely thank my wife Maria, who has always encouraged me and believed in my abilities, showing me every day how small wonderful things could become great, only with passion.

I am very thankful to my mother Marilena and my father Vittorino who, when I was a child, taught me how only honesty and respect for the others are the two milestones in human relationships, thus also in work. Unfortunately, these are not common human values.

List of Figures

Figure 1.1 The gecko's hierarchical adhesive apparatus. (A) Ventral view of the Tokay gecko (*Gekko gekko*). (B) Gecko's foot. Scanning electron microscope (SEM) micrographs of (C) the setae, (D) at higher magnification, (E) terminating in hundreds of spatula.

Figure 1.2 General scheme of a profile for the definition of the roughness parameters.

Figure 1.3 PMMA virgin surface. (A) Three-dimensional topography. (B) Two-dimensional profile (extracted at 50 μm from the edge of the square measured area).

Figure 1.4 Glass surface. (A) Three-dimensional topography. (B) Two-dimensional profile (extracted at 50 μm from the edge of the square measured area).

Figure 1.5 PMMA2400 surface. (A) Three-dimensional topography. (B) Two-dimensional profile (extracted at 50 μm from the edge of the square measured area).

Figure 1.6 PMMA800 surface. (A) Three-dimensional topography. (B) Two-dimensional profile (extracted at 50 μm from the edge of the square measured area).

Figure 1.7 Weibull statistics applied to the four data sets for G1 and in the case of moulting (X-dots) on virgin PMMA.

Figure 1.8 Weibull statistics applied to the four data sets for G1 and the two data sets for G2 (dashed lines) on glass.

Figure 1.9 Weibull statistics applied to the data set of G1 on PMMA2400 and to the two data sets of G2 on PMMA2400 and PMMA800.

Figure 1.10 Interpretation of experimental results for adhesion tests on various roughness of PMMA surfaces. (A) Setae (represented in blue) and sub-hierarchical structures (spatulae) can adapt well on virgin PMMA; (B) The adhesion on PMMA2400 is better because of the higher number of spatulae-substrate interactions; (C) On PMMA800, only partial contact interactions are achieved.

Figure 2.1 Spider and gecko feet showed by SEM (Zeiss EVO 50). The Tokay gecko (Fig.2.1F) attachment system is characterized by hierarchical hairy structures, which start with macroscopic lamellae (soft ridges ~ 1 mm in length, Fig.2.1H) and branches into setae (30-130 μm in length and 5-10 μm in diameter, Fig.2.1I, 2.1L (Hiller, 1968; Ruibal, 1965; Russell, 1975; Williams, 1982)). Each seta consists of 100-1000 substructures called spatulae, the contact tips (0.1-0.2 μm wide and 15-20 nm thick, Fig.2.1M (Hiller, 1968; Ruibal, 1965)) responsible for the gecko's adhesion. Terminal claws are located at the top of each singular toe (Fig.2.1G). Van der Waals and capillary forces are responsible for the resultant adhesive forces (Autumn, 2002a; Sun, 2005a), whereas the claws guarantee an efficient attachment system on surfaces with very large roughness. Similarly, an analogous ultrastructure is found in spiders (e.g. *Evarcha arcuata* (Kesel, 2003)). Thus, in addition to the tarsal claws, which are present on the tarsus of all spiders (Fig.2.1C), adhesive hairs can be distinguished in many species (Fig.2.1D, 2.1E). Like for insects, these adhesive hairs are specialised structures that are not restricted only to one particular area of the leg, but may be found either distributed over the entire tarsus - as for lycosid spiders - or concentrated on the pretarsus as a tuft (scopula) situated ventral to the claws (Fig.2.1A, 2.1B) - as in the jumping spider *Evarcha arcuata* (Kesel, 2003).

Figure 2.2 Weibull statistics (F is the cumulative probability of detachment/failure and t_i is the measured adhesion time) applied to the measured adhesion times on PMMA surfaces. PMMA 1 (red lines, for which we made 4 sets of measurements on four different days with gecko G1), PMMA 2 (dotted lines, for which we made 2 sets of measurements on two different days, one with gecko G1 (red) and one with gecko G2 (blue)), and PMMA 3 (blue double-line, for which we made the measurements in a single day with gecko G2).

Figure 2.3 A simple interpretation of our experimental results on the adhesion tests for living geckos on PMMA surfaces with different roughness. (A) Setae cannot adapt well on PMMA 1; (B) On PMMA 2, the adhesion is enhanced because of the higher compatibility in size between setae and roughness; (C) On PMMA 3 only partial contact is achieved. On the right, we report the analysed three-dimensional roughness profiles for all three investigated surfaces (from the top: PMMA 1, 2 and 3).

Figure 3.1 The Tokay gecko's adhesive system was observed by FESEM (Zeiss SUPRA 40) (A, B) and by SEM (Zeiss EVO 50) (C, D). (A) Toe and FESEM micrograph of the setae (B). SEM micrograph of the setae (C) A nanoscale array of hundreds of spatulae (D).

Figure 3.2 The Tokay gecko's adhesive system was observed by FESEM (Zeiss SUPRA 40). (A) The Tokay gecko's toe. (B, C) The connection area between adjacent lamellae, localized perpendicular to the longitudinal axis of each digit, is covered by nanostructured hairy units; (D) at high magnification.

Figure 3.3 The Tokay gecko's adhesive system was observed by FESEM (Zeiss SUPRA 40). (A) The Tokay gecko's toe. (B, C) The edge of the gecko's toe is covered by nanostructured hairy units; (D) at high magnification.

Figure 3.4 The experimental Tokay gecko with adherent elastic cloth bandaging and metallic connection hook on the measurement platform.

Figure 3.5 Force-displacement measurement platform.

Figure 3.6 Normal adhesive force-displacement curves on PMMA surfaces after the first and second moults. Snapshots show five specific instants of the gecko's displacement at 0, 148, 273, 423, and 723 g of hanging weight (W is the applied weight, W_G is the gecko's weight, δ is the gecko's displacement, and δ_{MAX} is the gecko's maximum displacement).

Figure 3.7 Normal adhesive force-displacement curves on glass after the first and second moults. Snapshots show five specific instants of the gecko's displacement at 0, 148, 348, 423, and 648 g of hung weight (W is the applied weight, W_G is the gecko's weight, δ is the gecko's displacement, and δ_{MAX} is the gecko's maximum displacement).

Figure 3.8 AFM characterization of the PMMA surface.

Figure 3.9 AFM characterization of the glass surface.

Figure 3.10 Damage imposed by the adhesive tests: (A) Diffused inflammation of gecko toes; (B) The gecko's healthy foot, for comparison; (C) Small, thin wound located on the gecko's skin between one toe and the next.

Figure 4.1 (A) A schematic 3D representation of the measured angle between the opposing front and rear feet (β_F) and between the first and fifth toe (β_T) of each foot on inverted surfaces (inset adapted from Y. Tian, N. Pesika, H. Zeng, K.

Rosenberg, B. Zhao, P. M., K. Autumn, and J. Israelachvili, *Adhesion and friction in gecko toe attachment and detachment*, 19320-19325, PNAS, December 19, 2006, vol. 103, no. 51; Copyright (2006) National Academy of Sciences, U.S.A.). The Tokay gecko adhesive system observed using FESEM (Zeiss SUPRA 40) (B, C, D) and by SEM (Zeiss EVO 50) (E). The gecko's toe (B), FESEM micrograph of setae arrays (C), SEM micrograph of several setae (D) and nanoscale array of hundreds of spatula tips (E).

Figure 4.2 The measured angle β_f between the opposing front and rear feet on different surfaces (steel, aluminium, copper, PMMA, and glass).

Figure 4.3 The measured angle β_t between the first and fifth toe: on the aluminium surface for all legs (A), or for the FR leg on different surfaces (steel, aluminium, copper, PMMA, and glass).

Figure 4.4 From the multiple peeling theory (Sitti, 2003), the dimensionless force f versus adhesion angle α using experimental mean values for α_f and α_t (fitting parameters λ reported in Table 4.1).

Figure 5.1 Side (A) and top (B) view of the centrifugal machine used to measure the insects sSF (M1: passive rotating linchpin; M2: electric motor connected to M1 with a transmission belt; FC: frequency controller to set the M2 rotational speed; RA: rotational axis; C: camera; B1: external box; B2: internal small box where specimens were placed in; M: middle of the internal box; L: lamp; BC: bicycle computer; CW: counterweight).

Figure 5.2 Two subsequent frames from a video: before detachment, the insect stands still on the surface (A) and, one frame later, it is in the box corner (B). These frames are extracted from a preliminary video without the use of the small box (B₂).

Figure 5.3 AFM characterization of the (A) steel, (B) aluminium, (C) copper, and (D) Cp surfaces.

Figure 5.4 The adhesive structures of the legs of *Blatta Orientalis*. (a) Frontal and (b) lateral view of a leg and some detailed micrographs (c, d, e, f, g) (d is the claw tip diameter).

Figure 5.5 The sSF for each individual are grouped by surfaces.

Figure 6.1 FESEM microscopies of the tested PS surfaces.